Superconducting Integrated Submillimeter Receiver for TELIS

Valery P. Koshelets, Andrey B. Ermakov, Lyudmila V. Filippenko, Andrey V. Khudchenko, Oleg S. Kiselev, Alexander S. Sobolev, Mikhail Yu. Torgashin, Pavel A. Yagoubov, Ruud W. M. Hoogeveen, and Wolfgang Wild

***Abstract*—In this report an overview of the results on the development of a single-chip superconducting integrated receiver for the Terahertz Limb Sounder (TELIS) balloon project intended to measure a variety of stratosphere trace gases is presented. The Superconducting Integrated Receiver (SIR) comprises in one chip a planar antenna integrated with a superconductor-insulator-superconductor (SIS) mixer, a superconducting Flux Flow Oscillator (FFO) acting as Local Oscillator (LO) and a second SIS harmonic mixer (HM) for FFO phase locking. As a result of the FFO design optimization a free-running linewidth between 9 and 1.5 MHz has been measured in the frequency range 500–710 GHz resulting in phase-locking of 35 to 95% of the FFO power correspondingly. A new generation of the SIR devices with improved FFO performance and optimized interface between FFO and SIS/HM has been developed and comprehensively tested. As a result all required TELIS parameters were demonstrated. Phase-locked FFO operation over entire SIR channel frequency range has been realized, spectral resolution below 1 MHz has been confirmed by gas cell and CW signal measurements. An uncorrected double side band (DSB) noise temperature below 250 K has been measured with the phase-locked FFO. The intermediate frequency bandwidth 4–8 GHz has been realized. To ensure remote operation of the phase-locked SIR several procedures for its automatic computer control have been developed and tested.**

***Index Terms*—Phase-locked oscillators, submillimeter wave integrated receivers, superconducting integrated circuits.**

I. Introduction

TELIS (TErahertz and submm LImb Sounder) [1] is a cooperation between European institutes to build a three-channel balloon-borne heterodyne spectrometer for atmospheric research. Many atmospheric trace gases have their rotational transitions in the sub millimeter and THz range, yielding a very rich spectrum. Limb sounding results in very accurate vertical profiles.

All three TELIS receivers utilize state-of-the-art superconducting heterodyne technology and will operate simultaneously. The 500 GHz channel is developed by RAL (Rutherford Appleton Laboratories, UK) and will produce vertical profiles of BrO, ClO, O_3, and N_2O. The 1.8 THz channel is developed by DLR (Institute for Remote Sensing Technology, Germany) and will mainly target the OH radical. This channel will also measure HO_2, HCl, NO, NO_2, O_3, H_2O, O_2, and HOCl. Finally the 550–650 GHz Superconducting Integrated Receiver (SIR) channel is developed by SRON Netherlands Institute for Space Research and Institute of Radio Engineering and Electronics (IREE). This channel will measure profiles of ClO, BrO, O_3, HCl, HOCl, H_2O, and its 3 isotopologues, H_O2, NO, N_2O, HNO_3, CH_3Cl, and HCN.

TELIS is designed to be a compact, lightweight instrument capable of providing broad spectral coverage, high spectral resolution and long flight duration ($\sim$24 hours duration in a flight campaign). The combination of high sensitivity and extensive flight duration will allow evaluation of the diurnal variation of key atmospheric constituents such as OH, HO_2, ClO, BrO together will longer lived constituents such as O_3, HCl and N_2O. TELIS will fly with a Fourier transform spectrometer MIPAS-B developed by the IMK (Institute of Meteorology and Climate research of the University of Karlsruhe, Germany). The two instruments together will yield the most complete set of stratospheric constituents. The TELIS instrument serves also as a test bed for many novel cryogenic technologies; the qualification flight is foreseen in 2007.

II. SIR Channel Design

The optical front-end of TELIS [2], [3], [4] consists of a pointing telescope, calibration blackbody and relay optics, common for the three channels: 500 GHz, 550–650 GHz and 1.8 THz. Frequency separation between the channels is performed quasioptically, allowing simultaneous observations by all receivers. First, one linear polarization of the incoming signal is selected by a wire grid and is reflected into the 500 GHz channel. The part of the beam that passes the grid is split between the two other frequency channels by a dichroic filter. After splitting the three beams enter a custom designed liquid helium cooled cryostat. A number of off-set reflectors are used to interface the optics from the telescope to the cryogenic channels.

The receiver chip is placed on the flat back surface of the elliptical silicon lens (integrated lens-antenna) with accuracy 10μm, determined by the tolerance analysis of the optical system. The SIR cold channel optics includes also Martin-Puplett polarizing interferometer used as a SSB (Single Side Band) filter and a number of curved and fold mirrors, all located in the vacuum space of the liquid helium cryostat [2], [3], [4]. The layout of the optics is shown in Fig. 1. All SIR channel components (including input optical elements) are mounted on a single plate

Manuscript received August 29, 2006. The work was supported in part by the RFBR projects 06-02-17206, ISTC project # 3174, NATO SfP Grant 981415, and in part by the President Grant for Leading Scientific School 7812.2006.2.

V. P. Koshelets, A. B. Ermakov, L. V. Filippenko, A. V. Khudchenko, O. S. Kiselev, A. S. Sobolev, and M. Y. Torgashin are with the Institute of Radio Engineering and Electronics, Russian Academy of Science, Mokhovaya 11, 125009, Moscow, Russia and also with the SRON Netherlands Institute for Space Research, 9700 AV Groningen, the Netherlands (e-mail: valery@hitech.cplire.ru).

P. A. Yagoubov, R. W. M. Hoogeveen and W. Wild are with the SRON Netherlands Institute for Space Research, 9700 AV Groningen, the Netherlands (e-mail: P.A.Yagoubov@sron.rug.nl).

Color versions of one or more of the figures in this paper are available online at http://ieeexplore.ieee.org.

Digital Object Identifier 10.1109/TASC.2007.898622

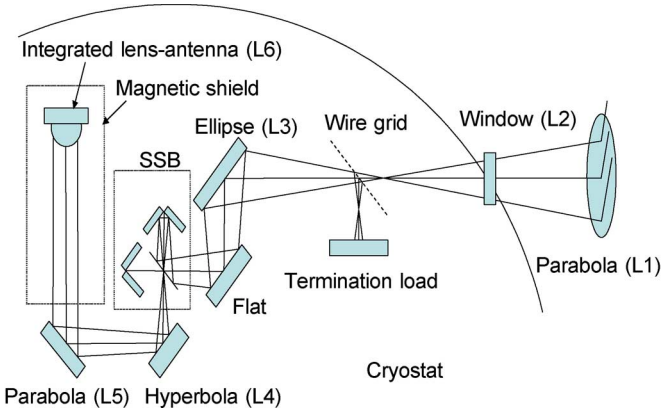

Fig. 1. Layout of the cold channel optics. Lines show the optical beam trajectories.

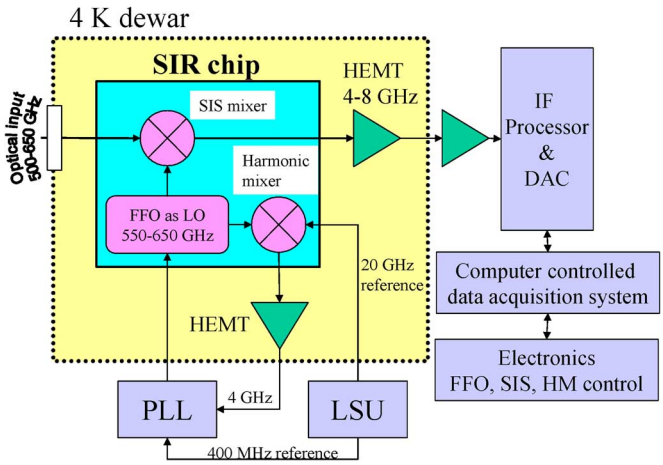

Fig. 2. Schematics of the SIR with phase-locked LO. FFO frequency is mixed in HM with the 19–21 GHz reference. The mixing product is amplified, down converted and compared with the 400 MHz reference in the PLL. The phase difference signal generated by PLL is used to feedback the FFO control line.

inside a $240\ \mathrm{mm} \times 180\ \mathrm{mm} \times 80\ \mathrm{mm}$ box cooled by the thermostraps to the temperature of about 4.2 K

A key element of the 550–650 GHz channel is the SIR [5], [6] that comprises in one chip (size of $4\ \mathrm{mm} * 4\ \mathrm{mm} * 0.5\ \mathrm{mm}$) a low-noise SIS mixer with quasioptical antenna, a superconducting Flux Flow Oscillator (FFO) [7]–[10], [11] acting as an Local Oscillator (LO) and a second SIS harmonic mixer (HM) for FFO phase locking, see Fig. 2. Since the free-running linewidth of the FFO can be up to 10 MHz, for spectral applications the FFO has to be locked to an external reference oscillator employing a phase lock loop system.

The concept of the SIR [5] looks very attractive for TELIS due to a wide tuning range of the FFO [7]–[10], [11]. Presently, the frequency range of the most practical heterodyne receivers is limited by the tunability of the local oscillator (LO). For a solid-state multiplier chain the fractional input bandwidth typically does not exceed 10–15%. In the SIR the bandwidth is basically determined by the SIS mixer tuning structure and matching circuitry between the SIS and FFO; bandwidth up to 30–40% may be achieved with a twin-junction SIS mixer design. To achieve the required instantaneous bandwidth of 550–650 GHz with emphasis on 600–650 GHz frequency range, a twin-SIS

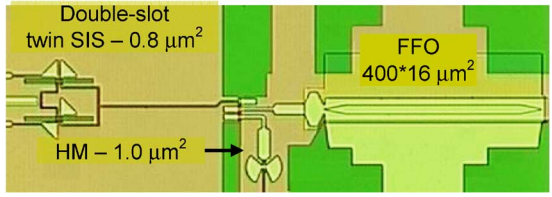

Fig. 3. Microphotograph of the central part of the SIR chip with double slot antenna.

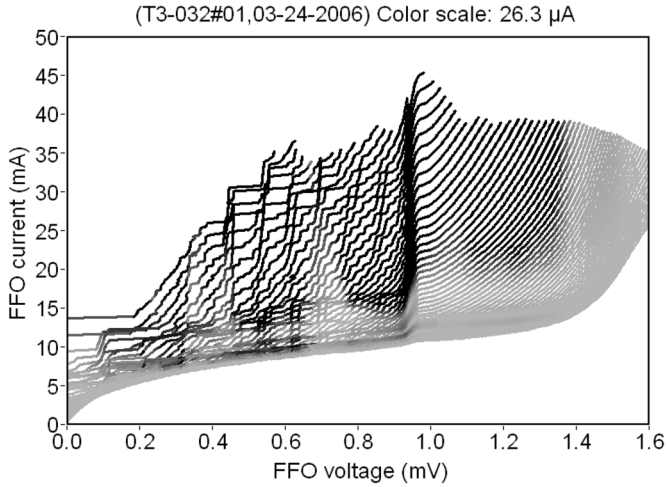

Fig. 4. IV-curves of the FFO ($\mathrm{length} = 400\ \mu\mathrm{m}, \mathrm{width} = 16\ \mu\mathrm{m}$) measured at different FFO CL currents; the pumping of the SIS-mixer is shown by gray scale (black color corresponds to pumping level >25% of SIS Ig), see Fig. 5.

mixer with 0.8 $\mu\mathrm{m}^2$ junctions and new design of the FFO/SIS matching circuitry were implemented. Microphotograph of the central part of the SIR chip with double slot antenna is presented in Fig. 3.

III. Optimization of the FFO for TELIS SIR

The FFO is a long Josephson tunnel junction in which an applied dc magnetic field and a bias current drive a unidirectional flow of fluxons, each containing one magnetic flux quantum. The velocity and density of the fluxons and thus the power and frequency of the emitted mm-wave signal may be adjusted independently by joint action of bias current and magnetic field produced by FFO control line (CL) current. There is a number of important requirements for the FFO properties to make it suitable for application in the phase-locked SIR. Obviously an FFO should emit enough power to pump an SIS mixer taking into account a specially designed mismatch of about 5 dB between the FFO and the SIS mixer, introduced to avoid leakage of the input signal to the LO path.

It is a challenge to realize the ultimate performance of separate superconducting elements after their integration in a single-chip device. Implementation of the improved matching circuits (Fig. 3) and submicron junctions for both SIS and HM allows to deliver enough FFO power optimal for the operation of these devices (see Figs. 4, 5, and 6). Note that the 19–21 GHz synthesizer provides pumping for HM while FFO power is a signal that should be down-converted, so even moderate HM pumping by FFO (5–10% of the HM Ig, where Ig is a current jump at the gap voltage Vg) is sufficient [11] to ensure large enough signal

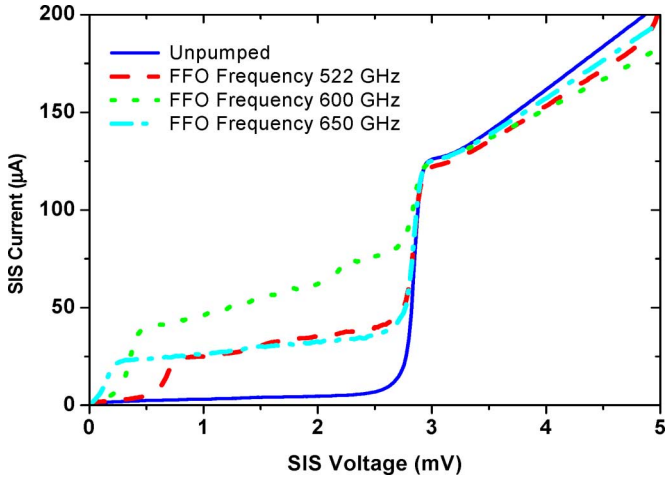

Fig. 5. IV-curves of the SIS-mixer: solid line—unpumped, dashed, dotted and dash-dotted—pumped by FFO at frequencies 522, 600 and 650 GHz correspondingly.

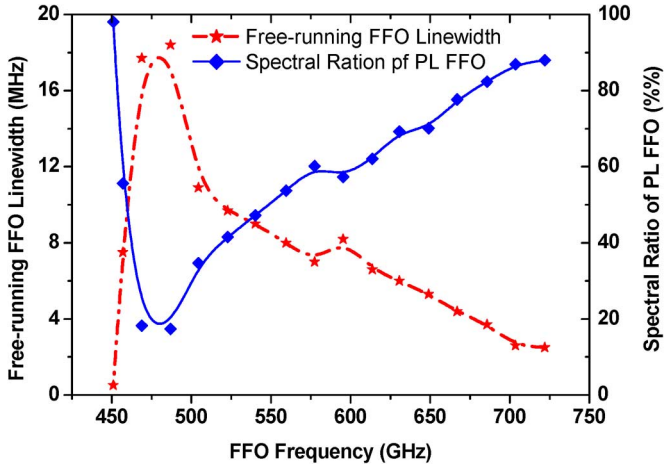

Fig. 7. Free-running linewidth and SR of PL FFO as a function of FFO frequency ($\mathrm{FFO\ width} = 28\ \mu\mathrm{m}$; $\mathrm{RnS} = 30\ \mathrm{Ohm} * \mu\mathrm{m}^2$).

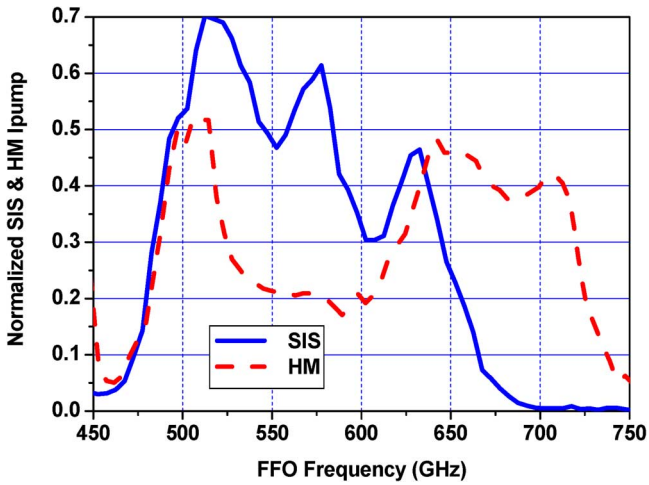

Fig. 6. Pumping of the SIS & HM mixers normalized on current rise at the SIS &HM gap as a function of FFO frequency at different FFO CL currents. The pumping level >25% of Ig ($> 26.3\ \mu\mathrm{A}$) is realized in the TELIS-SIR frequency range 500–650 GHz.

to noise ratio (SNR) at the IF output and consequently efficient FFO phase locking.

Even for an ultra wideband PLL system an effective regulation bandwidth is limited by the cabling length (about 12 MHz for typical PL loop length of two meters). It means that the free-running FFO linewidth has to be well below 10 MHz for stable FFO phase locking with a reasonably good spectral ratio (SR)—the ratio between the carrier power and the total power emitted by the FFO, which determines quality of FFO phase locking. For example, only about 50% of the FFO power can be phase-locked by the existing PLL system at the free-running FFO linewidth of 7 MHz. Low spectral ratio results in considerable error in resolving the complicated line shapes [6]. Thus sufficiently small free-running FFO linewidth is vitally important for realization of the phase-locked SIR for TELIS.

Previous measurements [11] have demonstrated a considerable increase of the FFO linewidth with FFO current density. It contradicts the simplified consideration: the increase of the FFO current density should result in the increase of the total FFO bias current, $\mathrm{I_B}$, and reduce the FFO differential resistance on the bias current $\mathrm{R_d}$. Since the FFO linewidth is proportional to $\mathrm{R_d^2} * \mathrm{I_b}$ one should expect the decrease of the measured FFO free-running linewidth for larger FFO current density. In reality $\mathrm{R_d}$ does not decrease as much as this simple consideration predicts and the linewidth increases. From the other hand high value of the current density ($\mathrm{J_c} \geq 8\ \mathrm{kA/cm^2}$) is important for wide-band operation of the SIS-mixer at the submm wave range. The discussed above increase of the FFO linewidth with current density creates serious problem in design and development of SIR chips. Implementation of two separate tri-layers with different current densities—one for the SIS mixer (high $\mathrm{J_c}$) and the other one for the FFO (lower $\mathrm{J_c}$) might be a solution. We have successfully tested and verified this approach for SIR TELIS microcircuits.

Dependences of the free-running FFO linewidth and SR of the phase-locked FFO on the FFO frequency measured at constant bias current of 32 mA are presented in Fig. 7. Abrupt increase of the linewidth at the FFO frequency of about 450 GHz is caused by the effect of Josephson self-coupling (JSC) [12]. The JSC considerably modifies FFO properties at voltages $\mathrm{V} \approx \mathrm{V_{JSC}} = 1/3 * \mathrm{Vg}$ ($\mathrm{V_{JSC}}$ corresponds to 450 GHz for a $\mathrm{Nb-AlO_x-Nb}$ FFO) and results in essential increase of the FFO $\mathrm{R_d}$ at voltages $\mathrm{V} > \mathrm{V_{JSC}}$ that significantly complicates phase locking of the FFO at the frequencies just above $\mathrm{e} * \mathrm{V_{JSC}}/\mathrm{h}$.

Recently it was shown [11] that for all frequencies of interest the linewidth can be considerably reduced by increasing FFO width, W, (consequently, the spectral ratio is getting much higher). We have further explored this approach by increasing the FFO width up to 28 μm (that corresponds to more than 5 times Josephson penetration depth λ_J). A number of FFOs with the same biasing electrodes layout but having tunneling regions of the different width ($\mathrm{W} = 4$, 8, 12, 16, 20 and 28μm) were fabricated using the same technological procedure with similar parameters (product of normal state resistance Rn and area S, $\mathrm{RnS} = 30\ \Omega * \mu\mathrm{m}^2$). The results of the linewidth measurements of these circuits at three FFO frequencies are presented in Fig. 8.

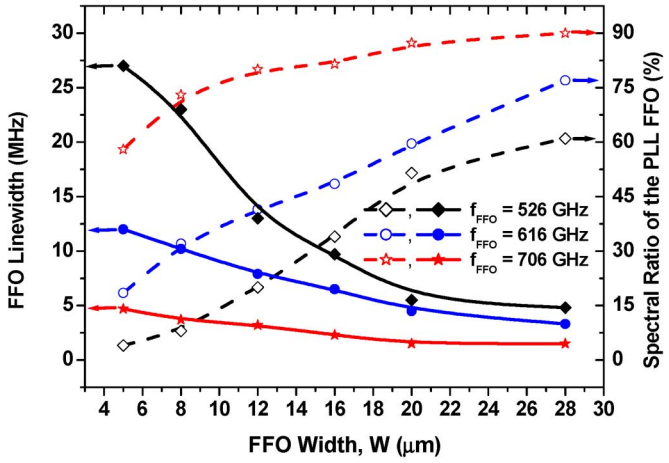

Fig. 8. Linewidth of free-running FFOs (left axis) and corresponding Spectral Ratio for the phase-locked FFO (right axis) measured at different FFO frequencies as a function of FFO width. All circuits are fabricated using the same technological procedure with similar parameters ($\mathrm{RnS} = 30\ \Omega * \mu\mathrm{m}^2$).

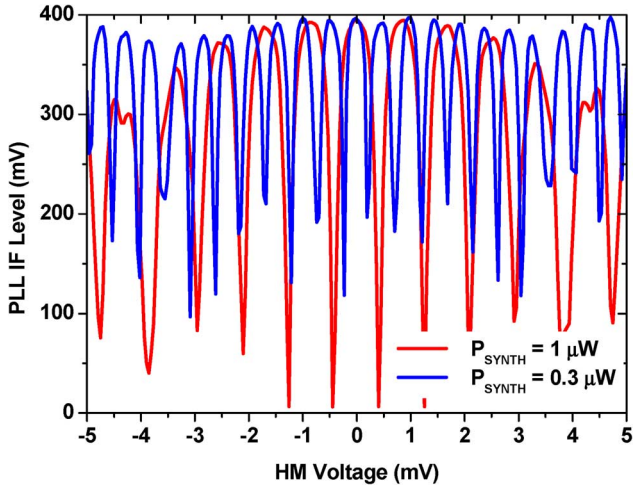

Fig. 9. A diagram for HM operational parameters measured by PC controlled PLL at 2 levels of synthesizer power delivered to HM (1 μW-solid line and 0.3 μW-dash-dotted line). Note that normal PL operation is possible at IF levels larger than 200 mV.

There is no evidence of deterioration of the FFO behavior even for the largest width tested ($\mathrm{W} = 28\ \mu\mathrm{m}$). Furthermore, the power delivered to the mixer is getting higher and linewidth smaller at all frequencies. The decrease of the FFO linewidth with the increase of the FFO width is quite explainable according to the existing theoretical models. $\mathrm{R_d}$ decreases more or less inversely proportional to $\mathrm{I_b}$ (in contrast to the case when we changed the FFO current density), and FFO linewidth has to go down linearly with the increase of the FFO width as $\mathrm{R_d^2} * \mathrm{I_b}$. Of course, one can expect to encounter a limit of the linewidth decrease and deterioration of the FFO behavior starting from some value of the width (for example, due to appearance of transversal modes). Since there is no reliable theory the optimal value of the FFO width has to be determined experimentally. Note that for a wide FFO there is a shift of the junction centerline from the edge of the FFO control line (assuming the same width of the idle region) that results in considerable decrease of the noise coming via magnetic field. Furthermore, a wider FFO provides, presumably, more uniform bias current distribution due to much smaller inductance of the overlapping electrodes in the FFO region.

An improved design of the FFO for TELIS has been developed and optimized. Free-running linewidth value from 9 to 2 MHz has been measured in the frequency range 500–710 GHz. As a result the spectral ratio of the phase-locked FFO varies from 35 to 90% correspondingly, ensuring that at least half of the FFO power is phase-locked in the primary frequency range for TELIS 550–650 GHz. The "unlocked" rest of the total FFO power increases the phase noise and the calibration error.

IV. Remote Optimization of the PL SIR Operation

It is important to ensure that tuning of a phase-locked SIR can be performed remotely. It is equally important to determine in flight the main parameters of the FFO at specific bias conditions (without complicated spectrum measurements). Knowledge of the spectral ratio of the phase-locked FFO is required for a correct retrieval procedure [11]. A computer controlled PLL system with a specially designed monitoring channel "IF level output" has been developed to adjust in the course of a flight the PL FFO operation (and to determine the resulting SR of the PL FFO) The dc signal at this output is proportional to the power measured by a detector with 0.8 MHz band-pass filter at 400 MHz. The DC signal from this detector is proportional to the PL FFO spectral ratio [11]; it means that SR can be determined in.

It is possible to optimize the HM tuning by monitoring the "IF level output" in the PL regime while the HM bias voltage and/or the synthesizer power are being adjusted (see Fig. 9) [12]. It is clear from Fig. 9 that there is a number of closely spaced local maxima. The height of these maxima is almost equal in a quite large range of parameters, so any of these peaks can be used for PL SIR operation. On the other hand the minima between the peaks are quite deep and precise tuning of the parameters (HM bias voltage, synthesizer power) is required. At lower synthesizer power delivered to HM (less than 1 μW) the spacing between peaks becomes twice as small compared to the optimum (see Fig. 9)—this corresponds to the crossover from the quasiparticle to Josephson mode of HM operation. No significant difference between these two regimes has been found; almost the same signal to noise ratio (SNR) and the same SR can be obtained. On the other hand the requirement to minimize cross talk between the pumped HM and the SIS-mixer forced us to use often the Josephson mode of HM operation for present PL SIR measurements. Note that all dependences are very well reproducible. Thus fine-tuning of HM operational regimes may be accomplished during the flight remotely by simple algorithms. It is important that the phase locking regime can be automatically restored if the HM mode is adjusted to one of the optimal peaks.

To realize the best receiver noise temperature the Josephson effect should be minimized. One of the SIS-mixer electrodes is used as an SIS control line (SIS_CL) [5]. A special procedure for remote suppression of the SIS critical current by computer tuning of the SIS_CL current has been developed and preliminary tested.

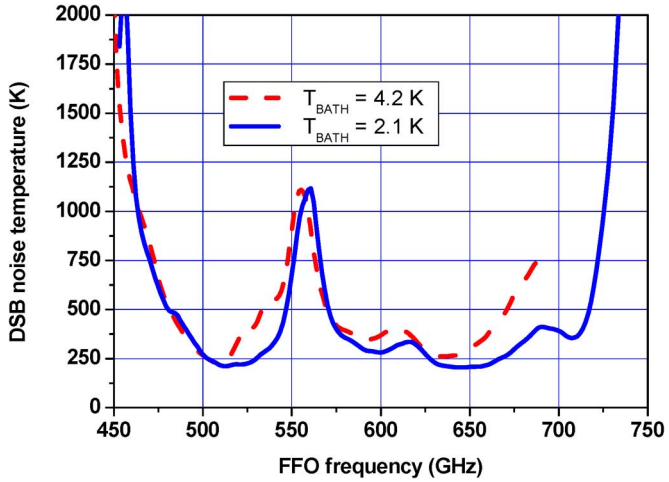

Fig. 10. Uncorrected DSB noise temperature of the SIR as a function of FFO frequency measured at different FFO bias currents to optimize the SIS pumping level: $T_{\mathrm{BATH}} = 2.1$ K (solid line), 4.2 K (dashed line), $\mathrm{V_{SIS}} = 2.2$ mV, IF = 4.3 GHz).

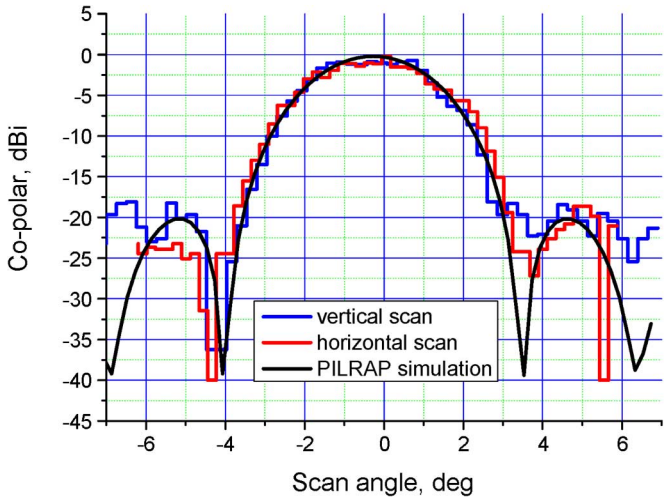

Fig. 11. Vertical (blue curve) and horizontal (red curve) far-field scans. The fit (black curve) is diffraction pattern calculated by PILRAP [15].

V. PL SIR Performance

The SIR microcircuits with modified design of the FFO-SIS/HM matching circuits have been tested as a receiver showing a possibility to realize the PL SIR concept. SIR chip is mounted in a flight configuration mixer block surrounded by a magnetic shield. No other optical elements of the cold channel were installed for the noise temperature and beam pattern measurements reported in this section. All tests were done in a liquid helium cooled cryostat.

A. Noise Temperature

Noise temperature measurements are done using Y-factor technique by chopping between hot (295 K) and cold (80 K) loads in the signal path of the receiver. IF response of the mixer is amplified by a cryogenic InP based 4–8 GHz low-noise amplifier (LNA) amplifier followed by a 60 dB gain GaAs room temperature amplifier. The signal is detected by a fast power meter in 40 MHz bandwidth, selected by tunable YIG filter. We have also used flight configuration of the PLL system and could lock the FFO practically at any frequency in the 550–650 GHz range.

The data were measured by specially developed data acquisition system for Integrated Receiver TEst and CONtrol (IRTECON) [13]. Usually such a procedure (for all frequencies of interest) takes about 15 minutes for any fixed SIS-mixer bias voltage (2.2 mV for data shown in Fig. 10). It was also possible to optimize the bias voltage of the SIS mixer for each FFO bias point; in this case a complete scan requires 1.5–2 hours. Note that there is a wide range of the FFO bias currents (i.e. FFO power) where Y-factor is close to a maximum; it makes possible to select the optimal conditions for HM operation. Rise of the SIR noise temperature at 557 GHz could be mainly explained by the strong absorption in the air due to the broad water line around this frequency. Vacuum hot/cold measurements are planned to be conducted in the future to exclude this effect from the measured results.

B. Integrated Antenna Beam Pattern

Far-field amplitude beam pattern of the integrated antenna has been measured at 625 GHz in a heterodyne mode with phase-locked FF0. The submillimeter source is a harmonic multiplier [14] driven by a microwave source. The dewar is placed on a rotation/tilt table to allow angular measurements. The tilt movement is referred to as the vertical scan and the rotation as the horizontal scan. The angle resolution of the system is 0.1°. The integrated antenna is located at the center of rotation. The measured beam pattern of the antenna is therefore expected to be independent on the beam pattern of the signal source. There are no focusing elements between the signal source and the receiver and the distance between them is about 70 cm. Signal source is positioned with ± 0.2 deg and ± 0.2 mm accuracy relative to the reference plane of the mixer block using He-Ne laser alignment system.

Results of the measurements for the double dipole antenna coupled SIR are shown in Fig. 11. The pattern is symmetric with the first sidelobe level below -17 dB. It is close to the theoretically predicted diffraction pattern calculated by PILRAP [15] and similar to the patterns measured with the double slot or double dipole antennas at these frequencies. The full width half maximum (FWHM) is 3 deg.

C. SIR IF Bandwidth

Forthcoming missions for the SIR require to have wide IF-band from 4 GHz to 8 GHz with flat characteristics over the band. Parasitic shunt capacitance of the SIS-mixer imposes fundamental limitations on the matching bandwidth of the IF circuitry [16]. For the SIR chip the shunting capacitance considerably increases due to a presence of the matching/coupling circuitry and on-chip RF-choke filters. The total capacitance added to the intrinsic capacitance of the mixer's tunneling AlOx barrier was estimated as 0.6 pF and 0.2 pF for the slot and the dipole-antenna designs correspondingly. The SIS normal resistance Rn can vary between 20 and 40 Ohm, depending on the RnS product of the tunneling barrier and the junction area; while the real part of the SIS-mixer impedance (which is the

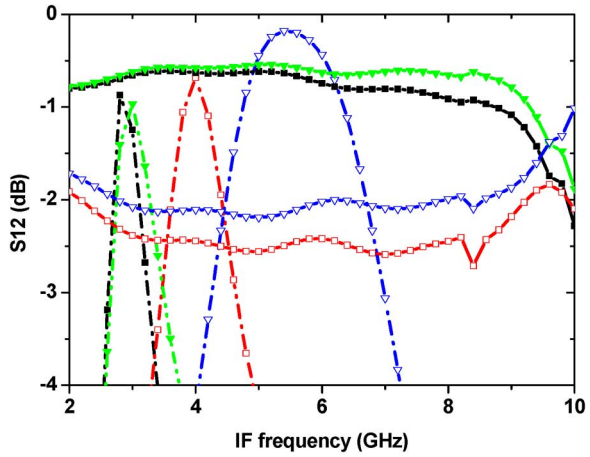

Fig. 12. Transmission characteristics S_{21} of the broadband (solid lines) and the narrowband (dashed lines) IF-networks. Symbols represent antenna type and Rp value. Solid bars—slot antenna at $\mathrm{Rp} = 20\ \mathrm{Ohm}$, empty bars—slot antenna at $\mathrm{Rp} = 150\ \mathrm{Ohm}$, solid triangles—dipole antenna at $\mathrm{Rp} = 20\ \mathrm{Ohm}$, empty triangles—dipole antenna at $\mathrm{Rp} = 150\ \mathrm{Ohm}$.

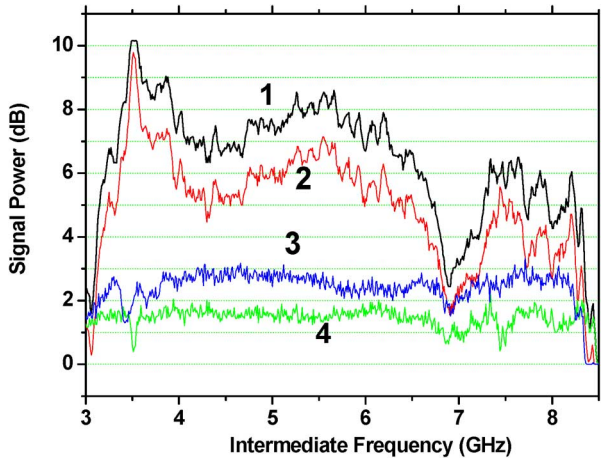

Fig. 13. IF spectra for the SIR with the slot antenna. Curve #1 and #2 are obtained at the hot (290 K) and cold (77 K) optical loads correspondingly; curve #4 is the difference between them. Curve #3—is the difference between IF spectra due to shot noise generated by the SIS biased at 10 mV and 4 mV.

input load for the IF-network) at any given operational point is the pumped differential resistance Rp on the SIS bias current. Its typical value is in the range 100–200 Ohm at voltages below the gap and determined also by the incident local oscillator (LO) power. The load impedance of the network corresponding to the cold amplifier impedance is assumed to be 50 Ohm.

A new approach to tune out the mixer's parasitic and filter's capacitances suggested by Jacob Kooi was implemented in a recently developed and tested IF-network for the SIR. A section of the coplanar line was grounded at RF by the integrated on-chip capacitors and worked as a shunt tuning inductance.

To make accurate adjustments of the layout parameters we use 2.5 D Sonnet simulator, which employs the Method-of-Moments and includes all parasitic, edge and cross-coupling effects that allow making an adequate representation of the bond wiring as well. In order to have a flat transmission characteristic of the network the coplanar line was divided into two sections that added an extra one tuning parameter. Fig. 12 shows Sonnet-simulated S21 characteristics of the entire IF-network designed for the two antenna types and extreme values of Rp (symbols with solid lines). Dashed lines correspond to the similar results obtained for the narrowband network of the previous old design, which provided a little lower noise temperature of the SIR, but was not suitable for many practical applications. Around some IF frequency points the narrowband network has almost 2 dB better transmission and therefore larger mixer gain compared to the new wideband design. Nevertheless we estimated from the receiver noise breakdown, that in the worst case extension of the bandwidth gives rise to the increase of the SIR noise temperature by 40–50 K in DSB.

The real performance of the new broadband matching network was tested for both antenna types. Fig. 13 shows IF spectra obtained for the SIR with the slot-antenna. Curve 3 is measured using the SIS tunnel junction (biased at $V > V_g$) as a perfect shot noise source with power proportional to the bias voltage with output impedance equal to R_d. Variations of the curves #1 and #2 are mainly determined by inhomogeneous gain of

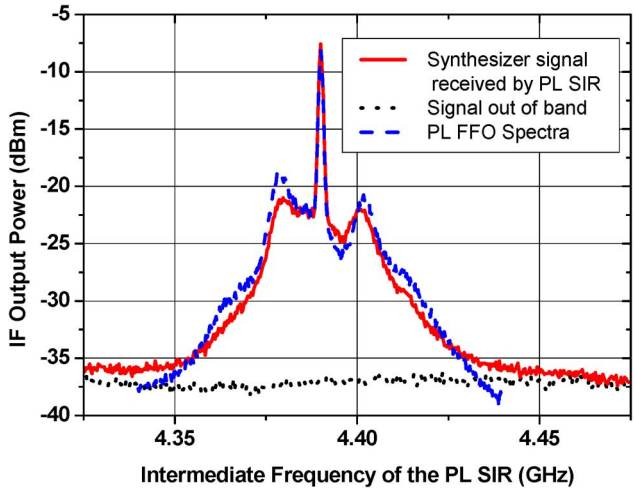

Fig. 14. Signal of multiplier driven by synthesizer ($17.967\ \mathrm{GHz} * 37 = 664.8\ \mathrm{GHz}$), measured by TELIS SIR with FFO phase-locked at 660.4 GHz-solid line. For the trace shown by dotted line the signal of the synthesizer is shifted by 5 MHz to be out of IF band. Dashed line—spectrum of the PL FFO, measured at HM IF output and frequency translated.

the amplifier's chain. The difference between the "hot" and the "cold" IF spectra (curve #4) is around 1.6 dB and weakly dependent on frequency and SIS mixer impedance—compare curves 3 and 4.

D. Spectral Resolution

To investigate frequency resolution of the receiver we have measured the signal of the synthesizer multiplied by a superlattice structure [14]. The results of these measurements are presented in Fig. 14; one can see that the signal recorded is a convolution of the delta-function provided by synthesizer with phase-locked spectra of the FFO with accuracy of the resolution bandwidth of the spectrum analyzer (1 MHz), so the frequency resolution of the receiver is not worse than 1 MHz.

To prove capability of the SIR for high-resolution spectroscopy we have successfully measured line profiles of OCS gas around 625 GHz. The tests were done in a laboratory gas

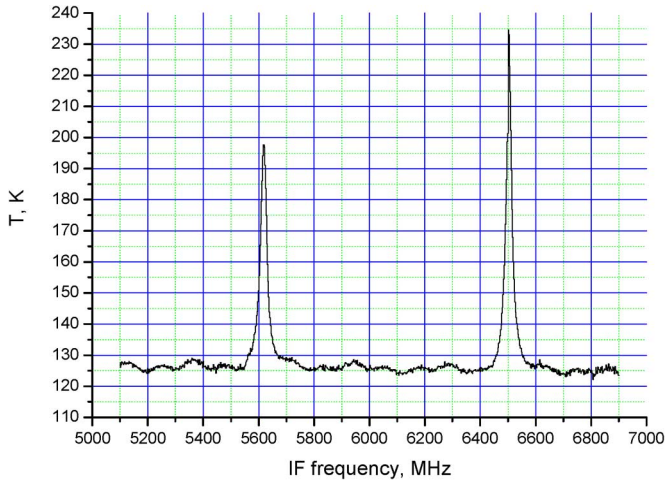

Fig. 15. Deconvolved spectrum of the OCS emission lines measured at different sidebands of the receiver at a gas pressure 1.2 mBar. LO frequency 625.24 GHz. Lines are saturated, the difference in line strength reflects the sideband ratio of the receiver.

cell setup at a gas pressure down to 0.2 mBar, corresponding to the FWHM linewidth <5 MHz. Gas cell measurements were done using a prototype cryostat, which accommodates complete cold channel. Only SSB filter was not installed at this moment to allow DSB operation of the receiver. For radiometric calibration we used room temperature (300 K) and liquid nitrogen (77 K) cooled blackbodies (Eccosorb). Switching between two calibration loads and a signal (gas cell) is done by a computer controlled flat mirror. As a back-end spectrometer we used Digital AutoCorrelator (DAC). SIR was operated in a phase-locked mode. Spectra are integrated from about 20 individual calibrated spectra. DAC integration time of individual spectrum is 1 sec. Recorded by the DAC spectrum is a convolution product of the signal (gas emission lines) with the FFO line spectrum, resolution is limited by DAC back-end. To recover the signal, we apply a simple direct deconvolution process using the measured FFO line shape.

For the measurements two OCS lines at 619.6213651 GHz and 631.7429035 GHz were selected. These lines could be observed at the same time, one in the upper and the other in the lower sideband of the receiver. The FFO was thus tuned at 625.240 GHz. The IF frequencies of these lines are 5618.6 MHz and 6502.9 MHz (see Fig. 15).

We have measured emission lines at different gas pressures, ranging from 0.2 mBar to 8 mBar. Example of the deconvolved spectrum at a gas pressure of 1.2 mBar is shown in Fig. 15. At this pressure both lines are expected to be saturated, pressure broadened and probably also saturation broadened; it was confirmed by measurements at higher gas pressures. One can note that the two lines have different strength. The difference in lines strengths reflects thus the sideband ratio of the receiver.

ACKNOWLEDGMENT

The authors thank Thijs de Graauw Gert de Lange and Avri Selig for fruitful and stimulating discussions, Sergey Shitov and Oleg Koryukin for participation in the initial stage of this work, as well as Vladimir Vaks, Oleksandr Pylypenko and Dimitry Paveliev for the development of the dedicated components for TELIS. We would be remiss, if we did not specially thank Jacob Kooi, who came up with the crucial idea on the improvement of the IF-match network and made many important comments on that.

REFERENCES

[1] R. W. M. Hoogeveen *et al.*, "New cryogenic heterodyne techniques applied in TELIS: The balloon borne THz and submm limb sounder for atmospheric research," in *Proc. of SPIE, Infrared Spaceborne Remote Sensing XI*, 2004, vol. 5152, pp. 347–355.

[2] P. A. Yagoubov *et al.*, "550–650 GHz spectrometer development for TELIS," in *The 16th International Symposium on Space Terahertz Technology*, Sweden, May 2005, pp. 438–443, Conference Proceedings ISSTT 2005.

[3] R. W. M. Hoogeveen *et al.*, "Superconducting integrated receiver development for TELIS," presented at the 12th International Symposium on Remote Sensing, Bruges, Belgium, September 19–22, 2005, unpublished.

[4] R. W. M. Hoogeveen *et al.*, "Sensors, systems, and next-generation satellites IX," in *Proc. of SPIE*, R. Meynart, S. P. Neeck, and H. Shimoda, Eds., 2005, vol. 5978, pp. 440–450.

[5] V. P. Koshelets and S. V. Shitov, "Integrated superconducting receivers," *Superconductor Science and Technology*, vol. 13, pp. R53–R69, 2000.

[6] V. P. Koshelets *et al.*, "Superconducting integrated receiver for TELIS," *IEEE Trans. Appl. Supercond.*, vol. 15, pp. 960–963, 2005.

[7] T. Nagatsuma, K. Enpuku, F. Irie, and K. Yoshida, "Flux-flow type Josephson oscillator for mm and submm wave region," *J. Appl. Phys.*, vol. 54, p. 3302, 1983.

[8] T. Nagatsuma, K. Enpuku, F. Irie, and K. Yoshida, "Flux-flow type Josephson oscillator for mm and submm wave region," *J. Appl. Phys.*, vol. 56, pt. II, p. 3284, 1984.

[9] T. Nagatsuma, K. Enpuku, F. Irie, and K. Yoshida, "Flux-flow type Josephson oscillator for mm and submm wave region," *J. Appl. Phys.*, vol. 58, pt. III, p. 441, 1985.

[10] T. Nagatsuma, K. Enpuku, F. Irie, and K. Yoshida, "Flux-flow type Josephson oscillator for mm and submm wave region," *J. Appl. Phys.*, vol. 63, pt. IV, p. 1130, 1988.

[11] V. P. Koshelets *et al.*, "Optimization of the phase-locked flux-flow oscillator for the submm integrated receiver," *IEEE Trans. Appl. Supercond.*, vol. 15, pp. 964–967, 2005.

[12] V. P. Koshelets, S. V. Shitov, A. V. Shchukin, L. V. Filippenko, J. Mygind, and A. V. Ustinov, "Self-pumping effects and radiation linewidth of Josephson flux flow oscillators," *Phys Rev B*, vol. 56, pp. 5572–5577, 1997.

[13] A. B. Ermakov, S. V. Shitov, A. M. Baryshev, V. P. Koshelets, and W. Luinge, "A data acquisition system for test and control of superconducting integrated receivers," *IEEE Trans. Appl. Supercond.*, vol. 11, no. 1, pp. 840–843, 2001.

[14] D. Pavel'ev *et al.*, "Temperature dependence of the radiation power emitted by a superlattice subject to a high-frequency electric field," in *Conference Digest of IEEE Joint 29th IRMMW-2004/12th THz-2004*, Karlsruhe, Germany, 2004, pp. 279–280.

[15] M. J. M. van der Vorst, "Integrated Lens Antennas for Submillimeter-Wave Applications," PhD thesis, Elect. Eng. Dept., Eindhoven Univ. Technol., Eindhoven, The Netherlands, 1999.

[16] J. W. Kooi, F. Rice, G. Chattopadhyay, S. Sundarum, S. Weinreb, and T. G. Phillips, "Regarding the IF output conductance of SIS tunnel junctions and the integration with cryogenic InP MMIC amplifiers," in *10th International Symposium on Spave TeraHertz Technology*, Virginia, March 1999, Univ. Virginia.